

IN-PLANE SEISMIC BEHAVIOUR OF SLENDER REINFORCED MASONRY SHEAR WALLS: EXPERIMENTAL RESULTS

B. Robazza¹, K.J. Elwood², D. L. Anderson³ and S. Brzev⁴

¹ Master's Student, Department of Civil Engineering, University of British Columbia, Vancouver, BC, V6T 1Z4, Canada, brook.robazza@civil.ubc.ca

² Associate Professor, Department of Civil Engineering, University of British Columbia, Vancouver, BC, V6T 1Z4, Canada, elwood@civil.ubc.ca

³ Professor Emeritus, Department of Civil Engineering, University of British Columbia, Vancouver, BC, V6T 1Z4, Canada, dla@civil.ubc.ca

⁴ Faculty, Department of Civil Engineering, British Columbia Institute of Technology, Vancouver, BC, V5G 3H2, Canada, Svetlana_Brzev@bcit.ca

ABSTRACT

Reinforced concrete block masonry shear walls (RMSWs) often constitute the principal seismic force resisting system of masonry structures. During an earthquake, these walls experience the combined effects of gravity axial loading and in-plane overturning moments due to lateral seismic forces. This may precipitate an out-of-plane instability, especially when the vertical reinforcement in the wall end zones is subjected to cycles of high tensile strain. This failure mechanism forms the basis of the current height-to-thickness (h/t) ratio limits (ranging from 14 to 20) for ductile RMSWs stipulated by the Canadian masonry design standard CSA S304.1-04. A comprehensive two-phase research program is being conducted to investigate the key parameters associated with out-of-plane instability in RMSWs subjected to in-plane loading. The first phase involved the experimental testing of five full-scale reinforced masonry column-like specimens subjected to uniaxial cyclic tension-compression loading, which provided a valuable insight into the instability failure mechanism. The second phase of the program is currently in progress, and it consists of reversed cyclic testing of full-scale RMSW specimens. The paper focuses on the key findings of the experimental study for the first wall specimen, characterized by an (h/t) ratio of 27 exceeding CSA S304.1 limits, and its possible implications on the CSA S304 seismic design provisions.

KEYWORDS: reinforced masonry, concrete blocks, shear wall, out-of-plane stability, ductile performance, seismic loading

INTRODUCTION

CSA S304.1-04 [1] restricts RMSWs to (h/t) ratios of 14 to 20 to prevent the possibility of out-of-plane instability failure in these walls when subjected to in-plane seismic loading. These limits depend on the expected seismic performance and the corresponding ductility-related force modification factor R_d stipulated by the National Building Code of Canada 2010 (NBCC 2010) [2] for different wall classes. The maximum R_d value of 2.0 corresponds to moderately ductile wall classes (note that $R_d = 1.0$ corresponds to elastic performance). For example, Moderately Ductile Shear Walls (height/length ratio of 1.0 and higher) are limited to a maximum (h/t) ratio of 14, and Moderately Ductile Squat Shear Walls are restricted to an (h/t) ratio of 20. NBCC 2010 requires that post-disaster buildings be designed with an R_d factor of 2.0 or higher

(irrespective of the level of seismic hazard), thus placing the most inhibitive restrictions on structures such as fire halls and police stations which used to be commonly built using RMSWs. A comprehensive literature review performed by Azimikor et al. [3] revealed an absence of experimental evidence related to out-of-plane instability in ductile RMSWs. Anderson and Brzez [4] provided a substantial explanation of the mechanism based on the findings of a study by Paulay and Priestley [5]. When a RMSW experiences considerable curvature ductility demand, large tensile strains develop in the vertical reinforcement in the tension end zone in the bottom portion of the wall. As this occurs, uniformly spaced flexural cracks of significant width begin to develop over the plastic hinge length. During the subsequent unloading cycle, the strains in the reinforcement reverse into compression. At this stage, the compression stresses in the wall are resisted solely by the vertical reinforcing bars, which may start to displace laterally due to limited lateral stiffness. At this stage, two mechanisms of response with different consequences are possible. The first mechanism develops if the flexural cracks close and the masonry in the end zone that was previously subjected to tension begins to resist compression; in that case, lateral stiffness of the compression region of the wall is restored and the wall remains straight. The second mechanism develops if the flexural cracks do not close before the lateral displacement reaches a critical value; in that case, the out-of-plane displacements may continue to increase, and out-of-plane instability may occur at the wall end zone.

Limited experimental evidence on the subject prompted the need for a research program which would characterize out-of-plane instability in RMSWs and develop rational criteria for out-of-plane instability in these walls. This paper describes the status and findings of a four-year, two-phase experimental program which has been undertaken by the authors of this paper in November 2010. Phase 1 of the program was focused on simulating the behaviour of the wall end zones using five full-scale reinforced masonry specimens with an h/t ratio of 27 subjected to uniaxial reversed cyclic loading. Note that these specimens were not able to simulate the actual boundary conditions along the height of the wall end zone, and did not take into account the effect of the strain gradient along the wall length, however the purpose of Phase 1 study was to understand the out-of-plane instability phenomenon and identify key factors which influence its development, as discussed by Azimikor et al. [6, 7]. The specimens exhibited out-of-plane displacements leading to lateral instability. A number of key factors were determined to precipitate the instability. It was observed that the mechanism heavily revolved around the development of large tensile yield strains in the vertical reinforcement prior to compression loading. The vertical reinforcement in the specimens underwent tensile strains on the order of 3.2 to $6.3\Delta_y$ before the out-of-plane instability occurred (where Δ_y denotes yield strain in steel reinforcement). It was observed that out-of-plane instability occurred when significant tensile strains developed in reinforcing bars across uniform horizontal cracks. These cracks were wide enough to cause the bars to act as though they were laterally unsupported. Once plastic tension strains developed in the reinforcement, compression stresses in the reinforcing bars would lead to out-of-plane displacements of the entire specimen, eventually triggering lateral instability once a critical tension strain was induced in a previous cycle. It was also found important that the reinforcement needed to be large enough to prevent local buckling before global instability could occur. Phase 2 of the program is in progress and consists of an experimental and analytical study of full-size RMSW specimens subjected to reversed-cyclic lateral loading. This paper describes the experimental testing program and presents the key research findings based on the testing of the first specimen.

SPECIMEN DESIGN AND CONSTRUCTION

Two identical full-scale wall specimens were constructed by a professional mason for the Phase 2 experimental study. The specimens are 2.6 m long and 3.8 m high (equivalent to 19 courses of masonry). The specimens were constructed using standard concrete blocks (400 mm length x 200 mm depth x 140 mm thickness) laid in running bond, and Type S mortar was used for face shell bedding. The vertical reinforcement consisted of one 15M reinforcing bar concentrated in the exterior two cells on each wall end, plus 10M bars spaced at 400 mm on centre along the wall length; this corresponds to the reinforcement ratio of 0.33%, which is similar to that used in Canadian design practice. The reinforcement was continuous up the wall height (no lap splices). The horizontal reinforcement was placed in bond beam blocks and consisted of 10M bars at 200 mm spacing (each course); this corresponds to the reinforcement ratio of 0.36%. Alternating 180° hooks were provided at the ends of horizontal bars. The specimens were fully grouted with a commercially available regular coarse grout mix. To ensure the wall stability during the construction, the grout was pumped in two lifts (one-half height and full height). The top three courses were constructed using wider, 190 mm blocks, and 10M vertical dowels as well as an additional horizontal 10M bar were provided to prevent sliding shear failure. The specimens were supported by 810 mm x 450 mm x 2660 mm (width x height x length) heavily reinforced concrete footing, with all wall vertical reinforcement fully developed in the footing. Wall specimen dimensions and the reinforcement layout are presented in Figure 1.

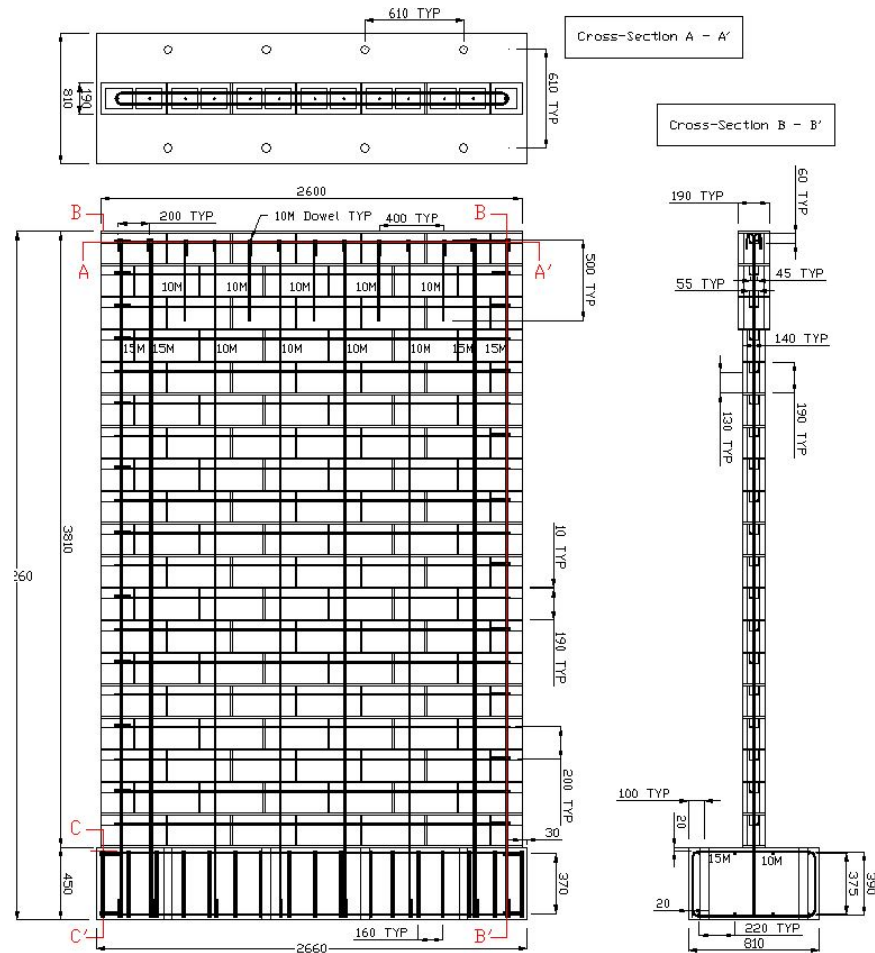


Figure 1: Wall specimen - dimensions and reinforcement details

The specimen height/length (h/l) ratio of 1.5 was chosen to ensure flexural behaviour characterized by the formation of plastic hinges at the base of the wall, a prerequisite for the out-of-plane instability. The wall height/thickness (h/t) ratio of 27, significantly higher than the upper CSA S304 limit, was chosen to increase chances for out-of-plane instability. The vertical reinforcement distribution was determined considering the criterion to maximize the length of the compression zone, and the corresponding strains in concentrated 15M reinforcing bars at the wall ends. The capacity design approach was followed to avoid the possibility of shear failure in the specimen.

Masonry material testing was performed following the procedures outlined in pertinent Canadian standards: CSA A165-04 for block testing, and CSA A179-04 for mortar and grout testing. Average compressive strength for the blocks was 53.8 MPa for the net area, based on 5 specimens. Type S mortar was used, with the average compressive strength of 12.4 MPa (based on 18 cubes). The average grout compressive strength was 35.4 MPa (based on 13 cylinders). The average value for the masonry compressive strength, f_m , was 21.2 MPa, based on 10 two-block-high grouted masonry prisms. Grade 400 reinforcing steel with the nominal yield strength of 400 MPa was used. Tensile tests were conducted on 10M and 15M reinforcing bar specimens, and the average yield strength was 505 MPa. The average yield strain for all specimens was 0.3%. The specimens were prepared and tested according to CSA G30.18-M92 (R2002) standard.

TEST SETUP AND PROCEDURE

The test setup was custom designed for this study and it is shown in Figure 2. The top of the specimen was connected to a double-channel steel loading beam through vertical rods. The loading was applied through one horizontal and two vertical MTS actuators attached to the loading beam. One end of the horizontal actuator (capacity 1000 kN, ± 343 mm stroke) was bolted to a set of ends plates welded to the loading beam, with its centreline aligned at the second highest course of masonry, and the other end was attached to the strong wall in the UBC Structures Laboratory. Two "near vertical" actuators (capacity 645 kN, ± 305 mm stroke) were inclined at an approximately 13° angle with regard to vertical to reduce the size of the loading beam. These actuators were connected to the loading beam by two high-strength post-tensioned steel rods each through bearing plates at the ends of the loading beam. The footing was attached to the laboratory's strong floor by post-tensioning to produce a rigid base connection. Out-of-plane lateral displacements at the top of the specimen were restrained by two adjustable steel arms connecting the support columns and the top of the loading beam through pin connections.

The objective of the test setup was to simulate the effect of seismic loads on the lower portion of a 9 m high wall in a three-storey building (referred to as simulated wall in the paper). The vertical compression loading was held constant at 660 kN (corresponding to axial compressive stress of $0.086f_m$). Lateral load on the specimen was applied through the horizontal actuator in combination with the net horizontal load from the sum of the two vertical actuators. The overturning moment representing the loads in the upper stories of the simulated wall was created by combined the effects of lateral and vertical loads of the actuators. The loads in the vertical actuators were slaved to the load from the horizontal actuator by a linear relationship derived from equilibrium equations relating the simulated wall to the wall specimen. This relation is demonstrated in Figure 3.

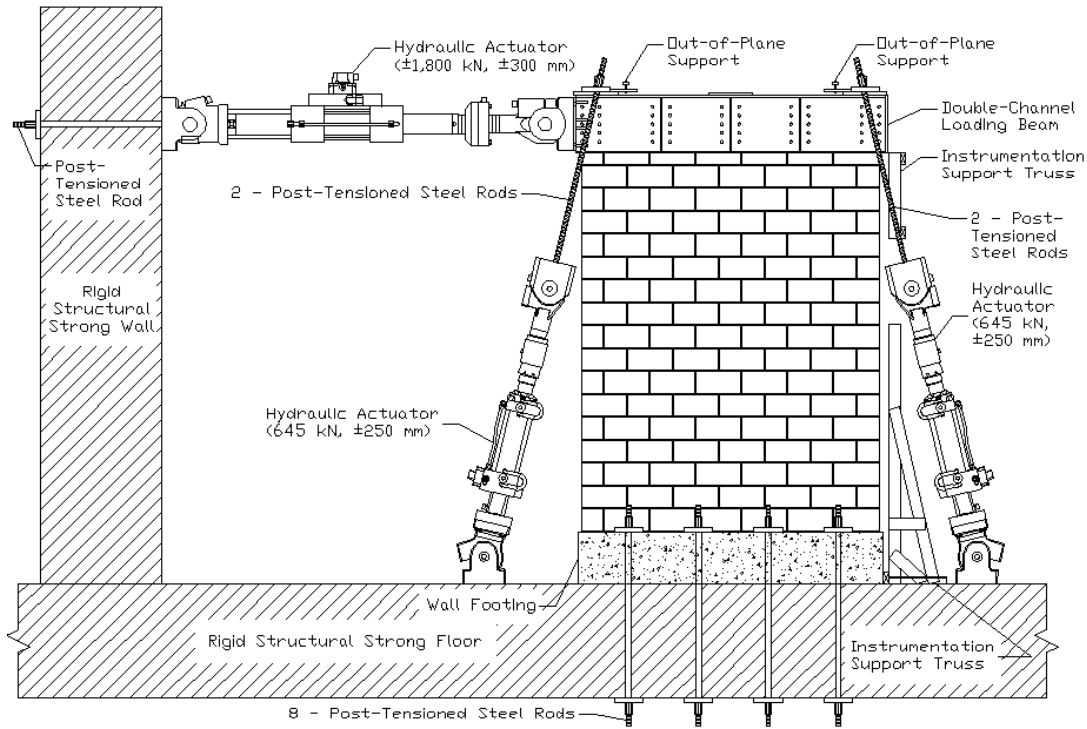


Figure 2: Test Setup

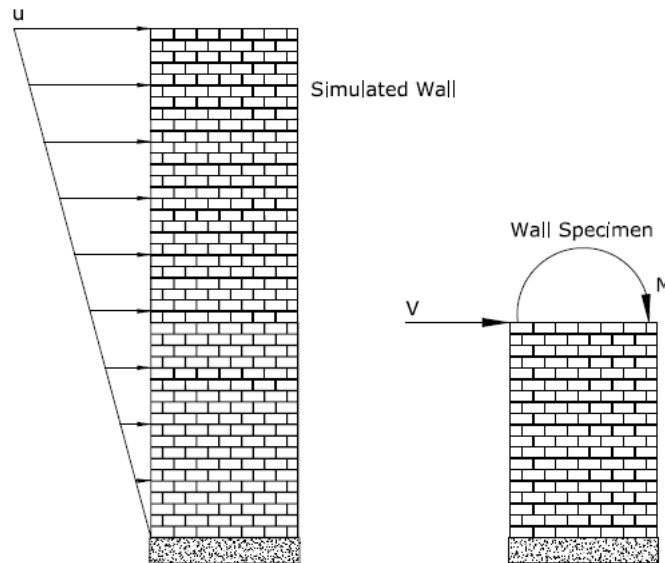


Figure 3: Applied lateral loads on the simulated wall and equivalent loads on the wall specimen

Loads and deformations in the specimen were monitored during the testing by a data acquisition system (Digital Equipment Station) with 53 channels. The instrumentation consisted of 21 string potentiometers and 16 linear potentiometers, which were used to measure vertical in-plane, horizontal out-of-plane, and diagonal in-plane deformations of the wall specimen, as shown in Figure 4. The configuration of these instruments created an effective strain rosette required to distinguish between flexural and shear deformations. Eight linear potentiometers were used to capture the out-of-plane displacements in the plastic hinge region, in-plane lateral displacements, uplift at the wall toes, base slip, slipping of the loading beam, and finally any lateral

displacements of the support columns due to potential loading from the out-of-plane supports. In addition, two inclinometers were utilized to capture the out-of-plane rotations of the plastic hinge region and 8 strain gauges were monitored strains in the 15M reinforcing bars at the wall ends.

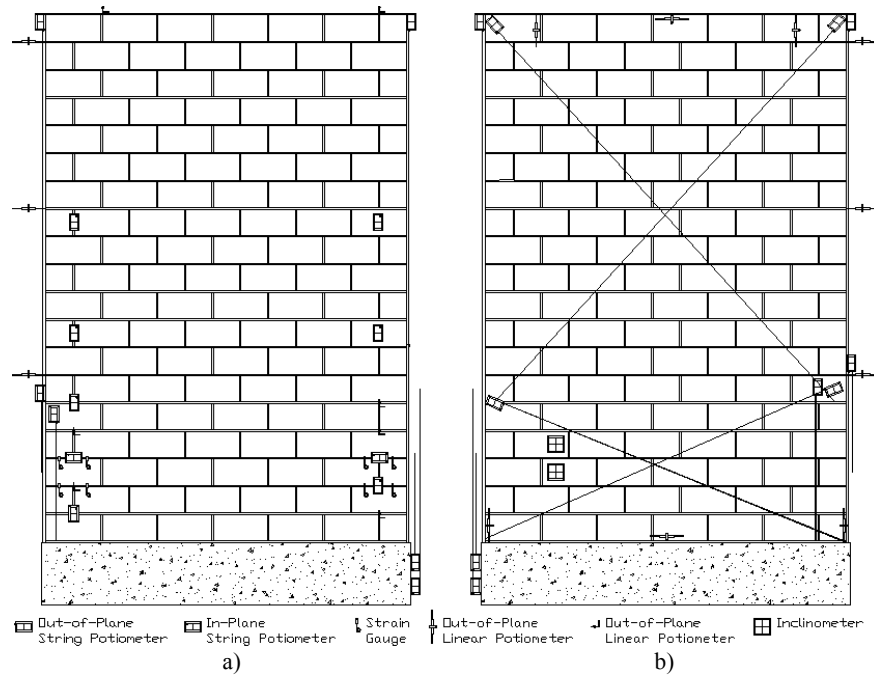


Figure 4: Test Instrumentation: a) West face, and b) East face

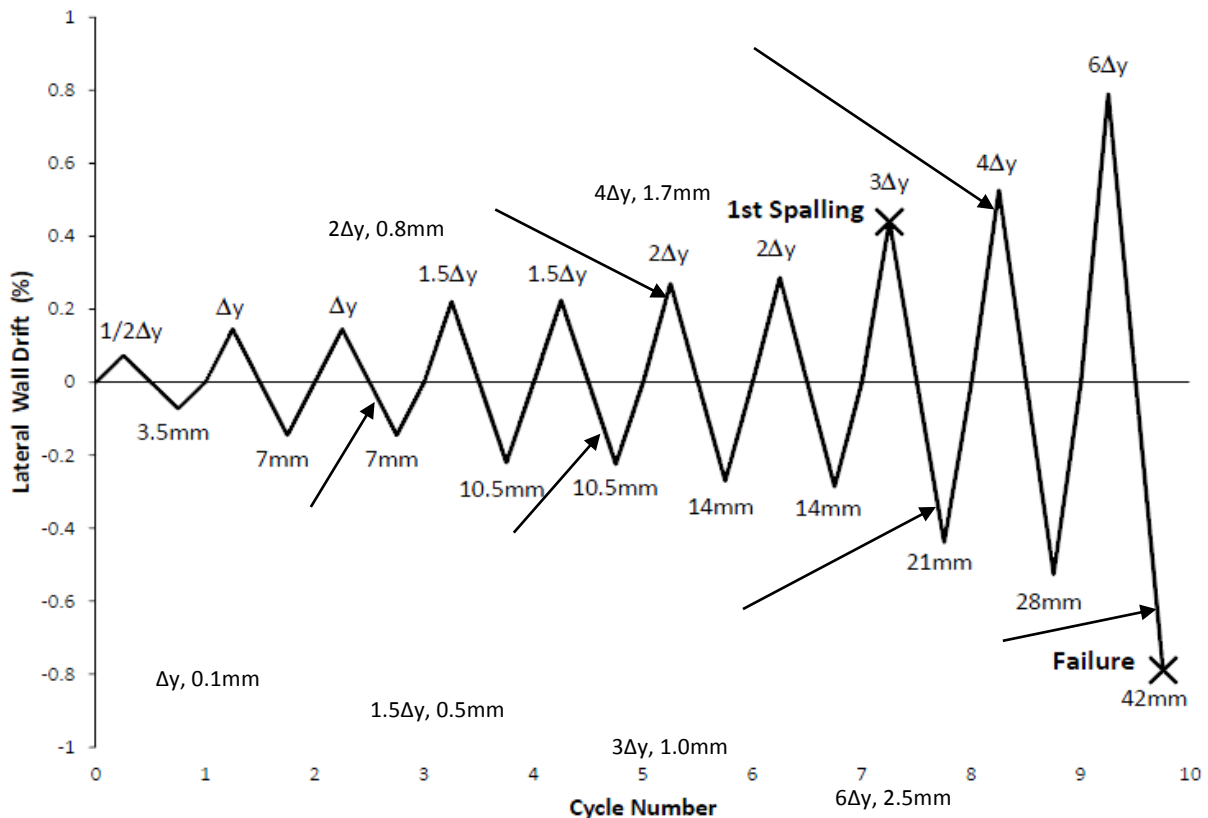


Figure 5: Loading protocol showing lateral wall drift on the y-axis, target actuator displacements and the corresponding maximum crack widths for each photo

The loading protocol is shown in Figure 5. The testing started after the initial vertical compression load of 660 kN had been applied by the near vertical actuators. The loading protocol was displacement-controlled, and it consisted of one or more cycles of incrementally increasing lateral displacements. The target displacement for each cycle was expressed in terms of Δ_y , the yield deflection in the outermost vertical reinforcing bars in the wall. The Δ_y value of 7 mm was determined by analysis and confirmed by the test data. It is important to note that the target displacement levels shown in Figure 5 were used by the controls during the testing; however, somewhat different displacement values are shown on the force-displacement hysteresis curves in Figure 10. This difference is due to gap closing within the test setup and the deflection of the strong wall.

TEST RESULTS

The specimen behaviour was elastic during the initial displacement cycles ($0.5\Delta_y$ and Δ_y). A number of cracks were observed at the Δ_y displacement level. The cracks were mapped at the end of each half-cycle (defined as the point of zero load). The cracks were located along the lower half of the wall specimen, and were mostly in the form of minor stepped cracks along the bed joints which originated at the wall ends. The maximum crack width of approximately 0.1 mm was observed along the bed joints. Figures 6 displays the crack pattern recorded during the test.

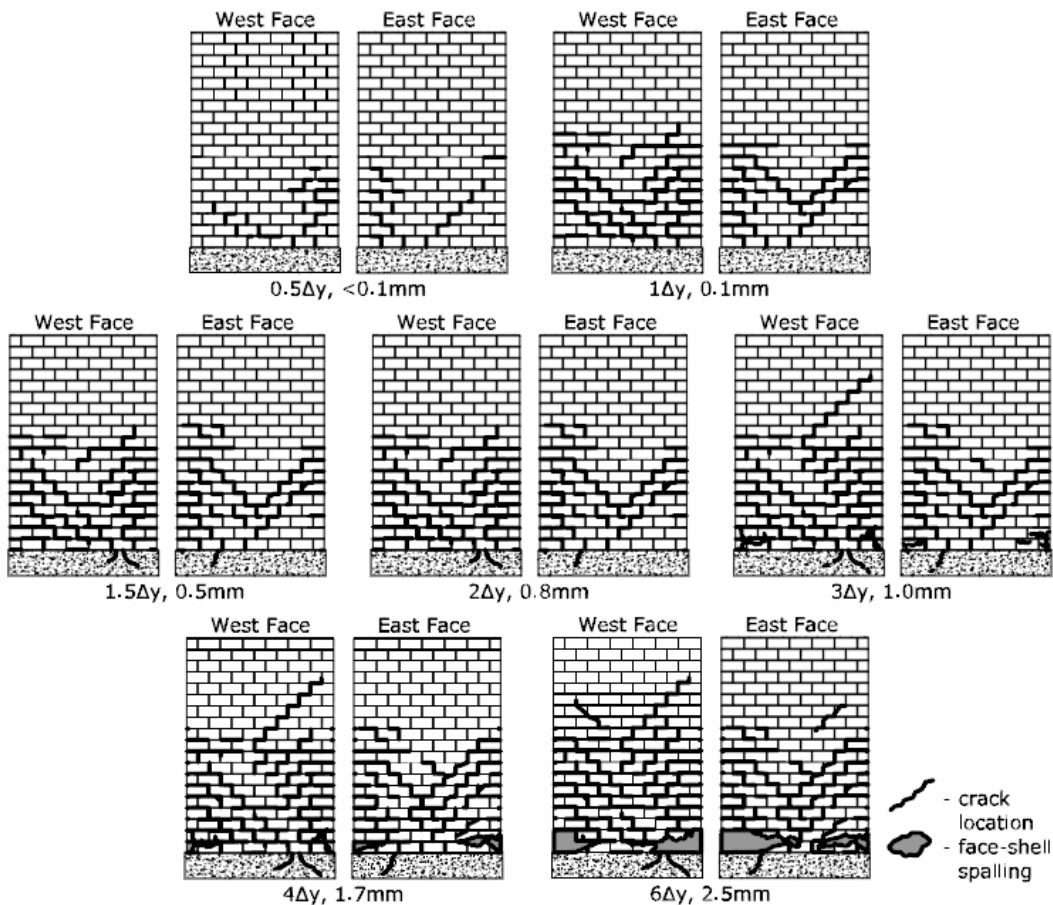


Figure 6: Cracking patterns at increasing target displacement levels

At the $1.5\Delta_y$ displacement level, the cracks observed at the end of the previous displacement cycle (Δ_y) further propagated, and a few new cracks were noticed. The cracking pattern remained primarily in the form of stepped cracks that originated at the ends of the specimen in its lower

half. There were two instances of diagonal cracks extending through the block units (see Figure 8), however most of cracking took place along the mortar joints. Maximum crack widths of 0.5 mm were observed at several locations at this stage.

During the $2\Delta_y$ displacement cycle, additional cracking occurred along the end faces of the wall, and relatively few mortar joints remained uncracked. Flexural horizontal cracks also began to open along the North and South faces, as well as along the base of the specimen. At this point, cracking was also observed in the footing but it was deemed not to affect the test results as the crack width remained below 0.3 mm throughout the test. Maximum horizontal and vertical crack widths of 0.8 mm and 0.1 mm, respectively, were measured along the existing cracks.

During the following cycle, the specimen was subjected to $3\Delta_y$ target displacement in the North direction. Extensive spalling developed at the North wall toe at the end of the cycle, as shown in Figure 7. The compression damage extended up the bottom two courses and resulted in a drop of 50kN (20% of peak) of the lateral load. The specimen behaviour was similar during the next half-cycle when the $3\Delta_y$ target displacement was applied in the South direction. The South wall toe also experienced face shell spalling, and the load dropped by approximately 50kN (20% of its respective peak) Cracks opened to a maximum width of approximately 1 mm along their horizontal lengths, and two new sets of step cracks were observed at the wall ends.



Figure 7: Cracking at the target displacement $3\Delta_y$: a) North toe, and b) South toe



Figure 8: Specimen damage at the target displacement $4\Delta_y$: a) North toe, and b) South toe

Spalling at the wall toes became more extensive during the target displacement $4\Delta_y$ cycle, as shown in Figure 8. The wall compression zone was shifted toward the centre because the toes crushed over the two bottom courses, and the vertical reinforcing bars at the wall ends were exposed. It was observed that the end reinforcing bars buckled under compression and

straightened under tension. The plastic hinge became apparent over approximately a 800 mm height starting at the wall base (bottom 4 courses). Cracking along the bed joints at the North and South wall ends extended up the lower 11 courses. Several major horizontal cracks were observed on the West and East wall faces, with the maximum widths of up to 1.7 mm.

The final target displacement load cycle of $6\Delta_y$ in both the North and South directions concluded the test. Loss of integrity of the wall toes became very significant at this stage, as shown in Figure 9. The specimen effectively lost the load-bearing capacity of approximately 1000 mm of wall length (nearly 40% of the overall wall length) due to the compression failure at the North end. It was observed from the spalled face shells that the interior face shell surface in contact with the grout was clean and smooth, which is a sign of poor bond. During the same half-cycle, the buckled reinforcement at the South wall end nearly straightened under tension. Cracks along the horizontal bed joints opened to a maximum 2.5 mm width, while the vertical crack widths remained within the 0.3 mm range. Besides additional large cracks at the wall toes, a new stepping crack formed at the compression end in the upper portion of the wall. The specimen demonstrated similar behaviour during the subsequent displacement half-cycle in the South direction. At this stage, crushing occurred in the South wall toe subjected to compression, and the reinforcement at the North end straightened under tension. Near the end of this half-cycle, a major drop in the load of 115 kN (roughly 60% of this cycles peak load) was observed. This effectively constituted failure of the wall specimen. After unloading to zero lateral load, the presence of vertical loads caused crushing of the specimen near the base. It is estimated that an effective loss of the load-bearing capacity at the wall toes over five or more block lengths resulted in excessively high compressive stress (approximately $0.5f_m$) at the centre of the wall.



Figure 9: Specimen failure at the target displacement $6\Delta_y$: a) North toe, and b) South toe

The load-displacement hysteresis curves are shown in Figure 10. The curves were obtained by plotting the recorded lateral forces from the actuator load cell versus the displacement at the 18th course. Figure 10a) demonstrates that the specimen displayed stable and relatively symmetrical hysteretic behaviour until the maximum load, Q_u , of 250 kN had been reached (corresponding to the displacement cycle $3\Delta_y$). The corresponding drift ratio was 0.36%, and the displacement ductility ratio (μ) was 2.1. Note that the equivalent yield load, Q_y , was approximately determined from the hysteretic behaviour and supported by the strain gauge data. Figure 10b) shows the final three load cycles before the failure. It can be seen that a 20% drop in load occurred at the 0.52% drift level, and the corresponding μ value was 3.1. The maximum ductility ratio reached during the test was 4.6, and the corresponding drift ratio was 0.79%. Figure 11a) shows the hysteresis curves for overturning moment versus lateral displacement, which are very similar to the curves

shown in Figure 10a). Figure 11b) displays average strains in the exterior vertical reinforcement. Although the strain gauges detected steel strains on the order of 0.02%, corresponding to the displacement $10\Delta_y$, average end zone vertical strains calculated from the recorded displacements indicated much smaller average strains of $2\Delta_y$ over the entire wall height. However, it must be noted that the average vertical strain was highly concentrated at the bed joints.

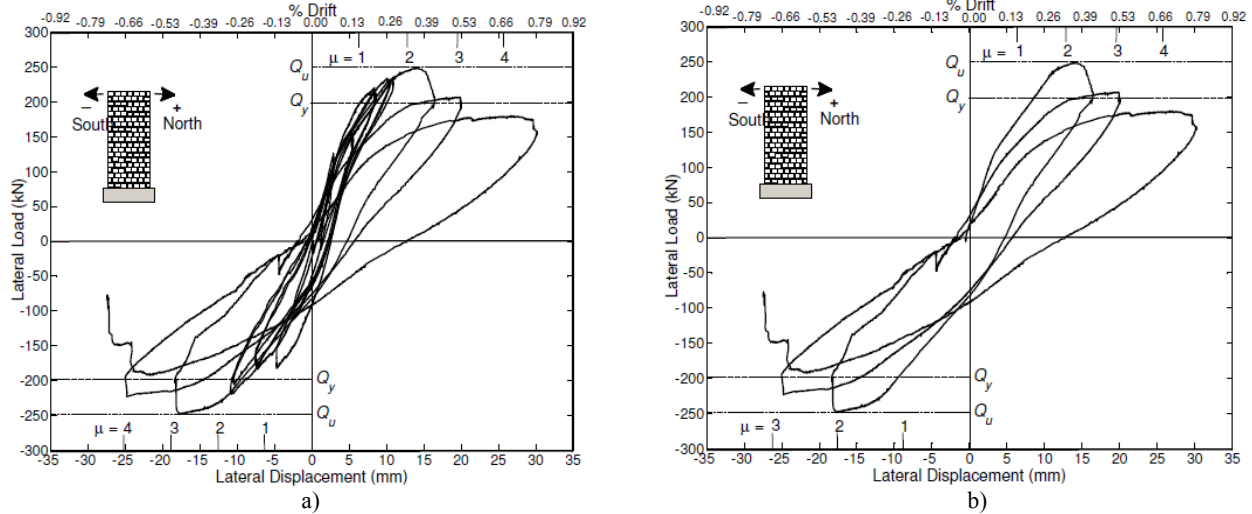


Figure 10: Lateral load-displacement hysteretic curves: a) full test, and b) last three cycles

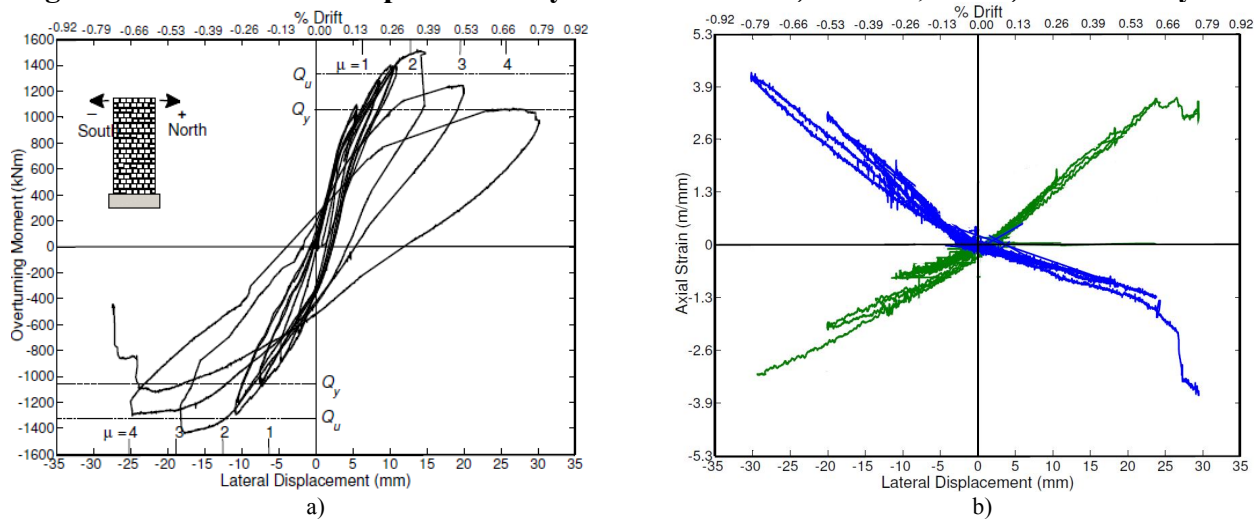


Figure 11: Hysteretic response of the specimen: a) overturning moment versus lateral displacement, and b) average vertical strains at the wall end zones

KEY OBSERVATIONS AND CONCLUSIONS

This paper outlines the behaviour of the first wall specimen tested in an experimental program designed to investigate the out-of-plane stability of RMSWs subjected to reversed cyclic in-plane loads. The following observations have been made based on the tests performed to date:

- Although both the specimen and the test setup were designed to create a behavioural preference for an out-of-plane instability mechanism, the failure occurred due to flexural compression (crushing) at the wall toes.
- An absence of the out-of-plane instability is possibly due to relatively large axial stresses in the specimen that were caused by applied vertical loads. These stresses prevented the horizontal flexural cracks from opening to widths large enough to facilitate instability. The

results suggest that the presence of high axial load may reduce the chances of lateral instability; however the effect of axial load will be further explored during the study.

- Buckling of laterally unsupported vertical reinforcing bars at wall ends was observed during the final loading cycles when the masonry disintegrated at the wall toes, however this did not precipitate global out-of-plane instability of the wall. These test results support the findings of Phase 1 study [6, 7], that is, the presence of uniform, wide flexural cracks along the plastic hinge length is critical for the occurrence of global out-of-plane instability. It appears that localized wall toe crushing may in fact prevent out-of-plane instability from occurring.
- High plastic tensile strains on the order of $10\Delta_y$ were recorded in vertical reinforcing bars at the wall ends during the test, however average strains over the wall height were significantly smaller ($2\Delta_y$). One of the findings of Phase 1 study was that high plastic tensile strain in the longitudinal reinforcement is the primary factor that determines the potential for out-of-plane instability in RMSWs. The effect of tensile strain needs to be further examined to determine its effect on the out-of-plane instability in RMSWs.
- The maximum ductility reached during the wall testing ($4.8\Delta_y$) was comparable to the ductilities achieved during the Phase 1 tests on uniaxial specimens which exhibited out-of-plane instability ($3.2 - 6.3\Delta_y$), and yet these tests resulted in different behaviour. This can be explained by the difference in strain gradient in the wall specimen and uniaxial specimens from Phase 1 study characterized by constant strain along the section.

ACKNOWLEDGEMENTS

The project was generously sponsored with funding from the Natural Sciences and Engineering Research Council of Canada under the Collaborative Research and Development Program, the Canadian Concrete Masonry Producers Association, and the Masonry Institute of British Columbia. Wall reinforcement was graciously donated by Harris Rebar Ltd. The invaluable assistance of the UBC and BCIT technicians and students was critical to the project's success.

REFERENCES

1. Canadian Standards Association, Masonry Design of Buildings (2004) CSA, S304.1-04, CSA Mississauga, Ontario, Canada.
2. NRC, National Building Code of Canada (2010) Institute of Research in Construction, National Research Council of Canada, Ottawa, Ontario, Canada.
3. Azimikor, N., Brzev, S., Elwood, K., and Anderson, D. (2011) "Out-of-Plane Stability of Reinforced Masonry Shear Walls", Proceedings of the 11th North American Masonry Conference, Minneapolis, MN, USA.
4. Anderson, D. and Brzev, S. (2009) "Seismic Design Guide for Masonry Buildings", Canadian Concrete Masonry Producers Association, Toronto, Ontario, Canada.
5. Paulay, T. and Priestley, M.J.N. (1993) "Stability of Ductile Structural Walls", ACI Structural Journal, Vol.90, No.4, pp.385-392, Farmington Hills, MI, USA.
6. Azimikor, N. (2012) "Out-of-Plane Stability of Reinforced Masonry Shear Walls under Seismic Loading: Cyclic Uniaxial Tests", a Thesis submitted in partial fulfilment of the requirements for the degree of Master of Applied Science, Faculty of Graduate Studies, University of British Columbia, Vancouver, BC, Canada.
7. Azimikor, N., Robazza, B., Brzev, S., Elwood, K., and Anderson, D. (2012). An Experimental Study on the Out-Of-Plane Stability of Reinforced Masonry Shear Walls Under In-Plane Reversed Cyclic Loads. Proceedings of the 15th World Conference on Earthquake Engineering, Lisbon, Portugal.